HHS Public Access

Author manuscript

J Nat Prod. Author manuscript; available in PMC 2017 March 25.

Published in final edited form as:

J Nat Prod. 2016 March 25; 79(3): 541–554. doi:10.1021/acs.jnatprod.5b00927.

Cycloartane Triterpenes from the Aerial Parts of *Actaea racemosa*

Ayano Imai[†,‡], **David C. Lankin**[†,‡], **Dejan Nikolić**[†,‡], **Soyoun Ahn**[†,‡], **Richard B. van Breemen**[†,‡], **Norman R. Farnsworth**[†,‡,§], **James B. McAlpine**[‡], **Shao-Nong Chen**[†,‡], and **Guido F. Pauli**[*,†,‡]

†

‡

Abstract

Investigating the phytochemical equivalence of the aerial parts of *Actaea racemosa* (*syn. Cimicifuga racemosa*) relative to the widely used roots/rhizomes, this study provides a perspective for the potential use of renewable ("green") plant parts as a source of black cohosh botanical preparations. In addition to the characterization of N_{ω}-methylserotonin as one representative marker of the *Actaea* alkaloids, nine cycloartane triterpenes were isolated and characterized, including the two new triterpene glycosides (1*S*,15*R*)-1,15,25-trihydroxy-3-O-β-D-xylopyranosyl-acta-(16*S*,23*R*,24*R*)-16,23;16,24-binoxoside (1) and 3-O-α-L-arabinopyranosyl-(1*S*,24*R*)-1,24,25-trihy-droxy-15-oxo-acta-(16R,23R)-16,23-monoxoside (2). Their structures were elucidated by spectroscopic data interpretation. The relative configuration of 1 was deduced by ^{1}H iterative full-spin analysis (HiFSA), making it the first example of the complete analysis of the complex ^{1}H NMR spectrum of a triterpene glycoside. In addition to the new compounds **1** and **2**, the aerial plant parts were shown to contain the previously known binoxosides **3, 4, 6,** and **7,** the monoxoside **8,** and the binoxols **5** and **9**. Overall, the metabolome of the aerial plant parts consists of a variety of *Actaea* triterpenes, similar to those found in roots/rhizomes, a tendency toward C-1 and C-7 hydroxylation of the cycloartanol skeleton, a greater abundance of aglycones, and the presence of comparable amounts of N_{ω}-methylserotonin.

Abstract

[*]**Corresponding Author** Tel: +1 (312) 355-1949. Fax: +1 (312) 355-2693. gfp@uic.edu..

[§]**Notes**

The authors declare no competing financial interest.

Supporting Information

The Supporting Information is available free of charge on the ACS Publications website at DOI: 10.1021/acs.jnat-prod.5b00927. NMR data for compounds **1** and **2** (1D ^{1}H, 2D ROESY/ COSY/HSQC/HMBC); 1D ^{1}H NMR data for known compounds **3**–**9** (PDF)

DEDICATION

Dedicated to Professors John Blunt and Murray Munro, of the University of Canterbury, for their pioneering work on bioactive marine natural products.

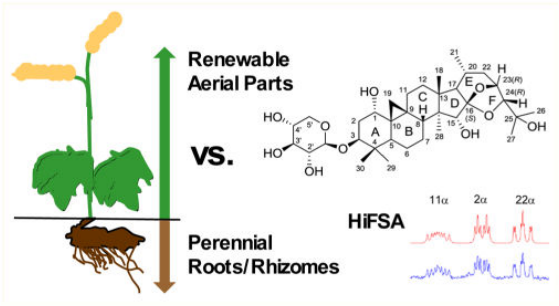

Black cohosh, *Actaea racemosa* L. (syn. *Cimicifuga race-mosa*), has been used widely as a dietary supplement for women's health. Historically, the crude plant material (roots and rhizomes) is sourced by collections of the whole plant, mostly from the wild. As a result, the growing demand for botanical products based on black cohosh is increasingly threatening the wild population of the plant.[1] The use of the aerial parts of black cohosh, however, could potentially alleviate this problem and represents an attractive alternative to serve as a renewable source for black cohosh dietary supplements, as the aerial parts may be harvested without sacrificing the entire perennial plant. A similar approach has been taken with another group of popular botanicals, ginseng (*Panax ginseng, P. quinquefolius*), of which the roots are the authentic plant material and the leaves are considered an adulteration. Ginseng roots also contain triterpene glycosides (ginsenosides), to which most of the pharmacological properties have been attributed. Although ginseng species are mainly supplied by cultivation, unlike black cohosh, effective usage of the aerial parts has been studied, e.g., *P. ginseng* leaves,[2] berries, and roots[3] for antihyperglycemic effects and *P. quinquefolius* leaves in the treatment of diabetes[4] as well as berries and leaves for anticancer activity.[5] The major phytoconstituents of black cohosh, the cycloartane triterpenes, are also contained in the aerial parts, albeit at lower concentrations than in the roots/rhizomes (10.5% and 23.5% in 70% aqueous MeOH extracts, respectively), as determined by quantitative ^{1}H NMR spectroscopy.[6]

Searching the Natural Products Alert (NAPRALERT) database provided a large number of studies associated with *A. racemosa* (52 citations and 117 compounds). However, none of the studies described any phytochemical work solely focused on the aerial parts. In 1965, Crum et al. screened plant species native to Ohio, including *A. racemosa*, for their alkaloid content using standard alkaloid screening and isolation procedures employing Dragendor?, Mayer, and Sonnenschein reagents.[7] However, information pertaining to the triterpene content of the aerial parts of black cohosh was not reported, even though triterpene glycosides represent a major class of the plant constituents.

An extensive search for other medicinally used *Actaea* (syn. *Cimicifuga*) species such as *C. simplex* (listed in the Japanese Pharmacopoeia) and *C. dahurica* (listed in both the Japanese and the Chinese Pharmacopoeia) revealed numerous studies of these species. Research results reported by Kusano et al.,[8] Liu et al.,[9] and Pan et al.[10] described the isolation of 40 compounds from the aerial parts of these species. Unique compounds were found in the aerial parts, and mutually distributed constituents were found in both the aerial parts and the

roots/rhizomes. In 2001, Kusano et al. reported on the differences in the isolated components between the roots/rhizomes and aerial parts, after analyzing a total of 66 cycloartane triterpene glycosides and their malonic ester derivatives.[8] While hydroxylations at positions 1α, 7β, and/or 12β are known to occur in triterpenes from aerial parts, no OH 7β-derivatives were isolated from the roots/rhizomes, but rather 7,8-didehydro derivatives were encountered frequently. Between initial submission and revision of this article, a report on the aerial parts of *Cimicifuga heracleifolia* (syn. A. *heracleifolia*) described 17 triterpene aglycones.[11] Of these, two C-24 epimers had 1-hydroxy groups that were assigned a β configuration on the basis of a ROESY correlation purportedly between H-1 and H-5, ignoring the fact that both H-5 and one H-2 had the same chemical shift. However, it is interesting that *A. heracleifolia* yielded only aglycones, despite a very polar extraction procedure, whereas *A. racemosa* gave predominantly glycosides. On the basis of previous studies of *A. racemosa* and other medicinal *Actaea* species, it was considered of interest to explore the chemical diversity of the aerial parts of A. racemosa and to determine the degree of similarity in the triterpene profiles between these two plant parts.

RESULTS AND DISCUSSION

Triterpene Glycosides from Aerial Parts of *A. racemosa*

Nine cycloartane triterpenes (1–9) were isolated from the aerial parts of *A. racemosa* for the first time. Among the isolates were two structurally new cycloartanes (1 and 2), and their structures were elucidated by combined 1D/2D NMR spectroscopy and LC-ESIMS. The new compounds were named in accordance with the recently proposed systematic naming system[12] for the *Actaea* cycloartane triterpenes as (1*S*,15*R*)-1,15,25-trihydroxy-3-O-β-D-xylopyranosyl-acta-(16*S*,23*R*,24*R*)-16,23;16,24-binoxoside (1) and 3-O-α-L-arabinopyranosyl-(1*S*,24*R*)-1,24,25-trihydroxy-15-oxo-acta-(16R,23R)-16,23-monoxoside (2). For comparison, in the old naming scheme, the compounds would be referred to as 1-α-hydroxy-24-*epi*-cimigenoside (1) and 1-α-hydroxydahurinol 3-O-α-L-arabinopyranoside (2), respectively.

In addition to the two new triterpenoids, two aglycones and five monoglycosides were isolated and characterized. While many aerial *A. racemosa* triterpenoids belong to the class of acta-16,23;16,24-binoxols (cimigenols), one of the prevailing constituents in *A. racemosa* roots/rhizomes, the spiroketal triterpenes, exhibited two distinctive characteristics in the aerial parts: (a) the unusual presence of aglycones and (b) the abundance of 1α-and/or 7β-hydroxylation. Even though seven of the triterpenes had been previously isolated from other *Actaea* species, five out of the seven triterpenes have not been isolated previously from the roots/rhizomes of *A. racemosa*. Along with the triterpenoids, three known flavanol glycosides were also isolated and characterized.

Whereas Kusano et al. have determined the configuration of the side chain of the acta-(16*S*,23*R*,24*R*)-16,23;16,24-binoxo-side skeleton by chemical means,[8] stereochemical characterization by NMR spectroscopy was not undertaken at that time. Using contemporary NMR instrumentation as enabling technology, the present study performed a detailed characterization of the side chain configuration by NMR methods, including HiFSA[13–15] and ROESY experiments.

Structural Analysis of the Glycosidic Residues

The pyranoside forms of xylose (xyl*p*) and arabinose (ara*p*) represent the predominant sugar moieties present in *Actaea* cycloartane triterpene glycosides. Evaluation of the full spin–spin coupling patterns of 1, 2, and 4 by HiFSA[7–9] (Table 1, Figure 1, NMR 1A, 1B) confirmed the respective aldopentose partial structures (C-1′ to C-5′) for the isolated glycosides. The xylp and arap pair of stereoisomers, in being epimeric at the C-4′ chiral center, affected the signal pattern of the protons at C-3′ and C-4′ and both methylene protons at C-5′. When elucidating the structure of the sugar moiety of an unknown Actaea triterpene, the protons H-5′α and β tended to give rise to the most suitable ^{1}H NMR marker signals. This is due to their cleanly observed multiplicity and appearance in a relatively uncrowded region of the spectrum. For the arap residue, the H-5′β proton signal appeared at higher field, as compared to that of H-5′α, and the pattern appeared as a pseudodoublet with a splitting of ~12 Hz. Upon closer inspection using the PERCH software tool for HiFSA, the signal for H-5′β appeared as a dd and exhibited a large ^2J coupling to its geminal partner, with a smaller ^3J vicinal coupling to H-4′. Proton H-5′α was also observed as a dd with coupling constants of 2.9 and −12.4 Hz. In contrast, the H-5′α signal of xylp appeared at higher field than the H-5′β as a pseudotriplet with a 9.5 Hz splitting. Precise measurement of this coupling was achieved by HiFSA, aflording coupling constants of 9.8 and −11.4 Hz. In this study, the carbohydrate moieties in the triterpene glycosides isolated from the *A. racemosa* aerial parts gave rise to H-5′ signals appearing in the range δ 3.55–3.80 ppm.

The chemical shifts of the H-5′ protons were highly affected by structural substitution in the aglycone. Substitution at C-1, for example, is commonly observed in *Actaea* triterpenes, and the effect on the chemical shift of the H-5′β proton, for example, by a hydroxy group here could be as large as Δδ 0.175 ppm, as seen when comparing 1 vs 8. In this study, the only two arabinosides were OH 1-analogues, and the H-5′β signals appeared around 3.66 ppm. It is not unusual for arap H-5′β signals to appear at ≤3.81 ppm. In this instance, signal multiplicity is a more reliable indicator than the $\Delta\delta$ values for identifying a key signal, because the chemical shift is strongly influenced by other factors such as the solvent, through-space shielding effects, and even conformational changes. Other interesting differences between xyl*p* vs arap residues are that in the ^{1}H NMR spectra of the former ^3J couplings between H and OH were observed, whereas they were absent in the arap residues. The H-2′ resonance in each residue illustrates this difference most vividly. In the arap-containing compounds, H-2′ is observed as a pseudotriplet and HiFSA yields a dd with J = 8.4, 7.1 Hz, indicating that it is spin-coupled to both H-1′ and H-3′, as expected. In contrast, H-2′ of the xylp moieties is observed as a “complex multiplet” and HiFSA revealed a ddd with J = 7.6, 8.8, 4.5 Hz, which indicates that H-2′ is also coupled to OH-2′ (^3J = 4.5 Hz) in addition to the expected couplings to H-1′ and H-3′. Such ^3J H–O–CH couplings were observed in all five xylopyranosides isolated in this study. In contrast, no ^3J HO–CH couplings were detected in the samples containing the arap residue. This suggests that the hydrogen-bonding networks present in the pentanopyranoid rings of these epimeric glycosides may be different, and this is, in turn, reffected in the differences observed in the ^{1}H NMR spectra of the two glycosidic residues.

Structure Elucidation of Compound 1

(1*S*,15*R*)-1,15,25-Trihydroxy-3-O-β-D-xylopyranosyl-acta-(16*S*,23*R*,24*R*)-16,23;16,24-binoxoside (1) was obtained as a colorless film. The HRESIMS revealed a sodiated molecule $[M + Na]^+$ at *m/z* 659.3743 (calcd for $C_{35}H_{56}O_{10}Na$, 659.3771), indicating a molecular formula for the sample of $C_{35}H_{56}O_{10}$. The 1D ^1H NMR spectrum revealed a pair of cyclopropane methylene protons at δ 0.447 and 0.729 ppm, six tertiary methyl singlets at δ 1.147, 1.186, 1.246, 1.262, 1.406, and 1.430 ppm, and a secondary methyl at δ 0.952 ppm. These data are consistent with this compound being a cycloartane triterpene, which is the characteristic compound class common to the *Actaea* species. In addition to the 1D ^1H NMR data, 2D COSY, HSQC, HMBC, and ROESY spectra were acquired.

A deshielded signal assigned to H-1_{eq} appeared at δ 3.825 ppm as a broadened singlet, suggesting the presence of a hydroxy group at C-1. The OH substituent at C-1 imparts a deshielding effect on H-11α and both C-2 methylene protons (δ 2.814, 2.741, and 2.272 ppm, respectively). The δ 3.5–5.0 ppm region of the ^1H NMR spectrum indicated that this compound has a single saccharide moiety, which was identified as a xylp unit exhibiting a diagnostic triplet for the H-5′α proton at δ 3.561 ppm. The COSY spectrum (Figure S2, Supporting Information) confirmed the correlations between each of the protons in the xylp ring. The ROESY spectrum (Figure S1, Supporting Information) showed correlations associated with the protons H-3/Me-29, H-1′/H-3, and H-1′/Me-29, confirming the attachment of the saccharide moiety at C-3.

The results of a phase-sensitive, multiplicity-edited HSQC spectrum (Figure S3, Supporting Information) allowed for the unambiguous assignment of the protonated carbons of 1. All quaternary carbons were assigned based on results of the HMBC spectrum (Figure S4, Supporting Information), with the exception of C-9 and C-10, as their cross-peaks were not observable due to limited sample availability (370 μg). However, when compared with the known compound (1*S*,15*R*)-1,15,25-trihydroxy-3-O-β-D-xylopyranosyl-acta-(16S,23R, 24S)-16,23;16,24-binoxoside, the ^1H and ^{13}C NMR chemical shifts of the ABCD rings were found to be almost identical. This only left the relative configuration of the side chain of the molecule to be deduced for this compound. The HMBC experiment revealed correlations between the carbon signal at 112.4 ppm, characteristic of a spiroketal carbon contained in a five-membered ring, with protons H-17 and H-15.[16] While these correlations confirmed that 1 possesses a spiroketal linkage at C-16, the ^1H NMR spectroscopic pattern for compound 1 did not match that of the structurally possible spiroketal compound (1*S*,15*R*)-1,15,25-trihydroxy-3-O-β-D-xylopyranosyl-acta-(16S,23R,24S)-16,23;16,24-binoxoside,[17] suggesting that 1 is a stereoisomer of this compound.

Configuration of the C-23 and C-24 Stereogenic Centers in 1

Initially, the configuration of 1 was determined by comparison of the ^1H NMR splitting pattern of the signals of the side chain spin system with that of an acta-(16S,23R, 24S)-16,23;16,24-binoxoside-type isolate (7S,15R)-7,15,25-trihydroxy-acta-(16S,23R, 24S)-16,23;16,24-binoxol (5; Figure 1C, D). The individual signal patterns for H-17, Me-21, H-22α, and H-22β and their corresponding J-couplings were identical to those of 5, even though they exhibited different ^1H NMR chemical shifts. Analysis of the signal for H-20

was limited by its complex multiplicity, which was further confounded by spectral overlap with signals arising from other protons. A noteworthy observation was that H-23 in 1 appeared as a ddd (J = 9.8, 2.3, 4.2 Hz), while H-23 in 5 appeared as a dd (J = 9.8, 2.3 Hz). Also, H-24 in 1 exhibited an additional coupling of 4.2 Hz when compared with the H-24 (singlet) in 5. The additional coupling between H-23 and H-24 in 1 relative to 5 suggested that the dihedral angle between H-23 and H-24 in compound 1 is different from that in 5, where the absolute configurations at C-23 and C-24 are 23*R*, 24*S*. Even though both 23R, 24*R* and 23*S*, 24*S* were considered as possibilities for having different dihedral angles between H-23 and H-24, the configuration was determined as 23R, 24R from the analysis of the spin coupling pattern. Examination of the H-22α and H-22β couplings to H-23 showed that 1 and 5 have identical coupling constants of 9.8 and 2.3 Hz, respectively, which suggests that the configuration of ring E in compound 1 is identical to that in compound 5. Hence, the relative configuration of the side chain is consistent with 23R, 24R.

HiFSA Analysis of Compound 1

The spin–spin coupling patterns in 1 were analyzed by ^{1}H iterative full-spin analysis (HiFSA)[7–9] using the PERCH software tool, and the results were fully consistent with the proposed structure of 1 (Figure 2). The ^{1}H NMR spectrum was resolution enhanced prior to analysis. The spin system was initially simulated in automation mode and then adjusted by fine-tuning the key NMR parameters (δ, J values) until the simulated and experimental spectra were superimposable. There are four independent spin systems present in 1 that were, for simulation purposes, treated independently. Table 2 summarizes the fully analyzed coupling patterns together with the chemical shifts and coupling constants for each individual spin system. HiFSA allowed identification of small couplings that might otherwise be overlooked. Specifically, this analysis revealed, for example, that the C-18 methyl signal is spin coupled to H-12β through four bonds with a small ^4J of 0.76 Hz. While the C-18 methyl has generally been assigned as a singlet in previous reports on *Actaea* triterpenes, the long-range coupling phenomenon has been reported in NMR studies of steroids.[18–22] Similarly, while the splitting of the Me-18 signal was not observed even at high magnetic field (900 MHz ^{1}H) with application of resolution enhancement, this ^4J coupling broadens the Me-18 signal compared to other methyl peaks, thus contributing to precise assignment of the Me-18 signal and distinction from other methyl signals. To assign unambiguously methyl ^{1}H signals, 1D ^{1}H NMR and 2D COSY experiments are by themselves insuficient, and HMBC experiments are necessary in most cases. Analogous observations likely apply to other cycloartanes lacking substitution at C-12. Although the Me-18 signal appears to be a singlet, it displays the lowest peak height and is the broadest ($W_{1/2}$) of all the tertiary methyl resonance peaks in the spectrum. The early work of Bhacca and Williams provides a comprehensive discussion of long-range couplings to angular methyl groups in steroids.[23]

Another long-range coupling of 0.80 Hz was observed between H-19 exo and H-5. This is typical of the ^4J coupling seen across bonds in a planar W arrangement. It is important to note that the H-19 *endo* proton does not exhibit a long-range coupling, which makes this pair of signals appear slightly different from one another, as shown in Figure 2. H-19 *exo* and H-19 *endo* are geminally coupled (^2J = 4.2 Hz), and H-19 *exo* exhibits an additional

coupling (^4J = 0.80 Hz) to H-5. Although this additional 0.80 Hz coupling was included in the HiFSA iteration of the H-19 *exo* signal, its signal intensity is about ~10% greater than the H-19 *endo* signal. The same phenomenon may be observed for other cycloartane isolates and suggests that, although only one long-range coupling (H-19 *exo*/H-5) was included for iteration, a number of small couplings (<0.8 Hz) not included in the iteration contribute to the signal line shape and intensity. This was confirmed by high-quality COSY spectra of related compounds (5 and 8). Unfortunately, the cross-peaks associated with the long-range couplings were not observed in the COSY spectrum of **1**, because of insuficient signal-to-noise arising from a low sample concentration. However, the cross-peak patterns observed for **5** and **8** were similar to that of **1**, and the following may be suggested generally for cycloartane-type triterpenes. Mutually observed cross-peaks were H-19 *endo*/H-1a, 8,11a and H-19 *exo*/H-5, **8**. The cross-peak between H-19 *endo* and H5 was observed in 5, but not in 8. This illustrates that high-quality COSY spectra have the potential for revealing long-range ^4J–^5J couplings. Proton H-1β was observed at δ 3.825 ppm (lower field) as a broadened singlet due to coupling of the OH at C-1 to H-1β. HiFSA iteration revealed that H-1β is actually a ddd and that it is coupled to H-2α, H-2β, and OH-1 with J = 3.65, 2.70, and 3.67 Hz, respectively.

^{1}H NMR Substituent Chemical Shift (SCS) effects in 1

The inverted configuration at C-24 forces the tertiary alcohol moiety to be folded behind the E ring instead of pointing away from the E and F rings (Figure 3). Significant relocation of the C-25(OH) introduces shielding/deshielding SCS effects on the neighboring proton resonances, which range from a $\delta\Delta$ as small as 0.06 ppm to as much as 1.63 ppm. In general, the protons residing behind the E ring tend to be deshielded. For example, the chemical shifts of H-22α, H-17, Me-21, and H-20 were shifted downfield by 1.63, 0.23, 0.07, and 0.06 ppm, respectively, in the spectrum of 1 compared to their positions in that of 5, while the chemical shifts of protons H-22β, H-23, and H-24 were shifted upfield by 0.37, 0.20, and 0.12 ppm, respectively. The methylene protons of C-22 experienced significantly different effects as a result of the inverted configuration. The signal associated with H-22α appears downfield relative to that of H-22β in the spectrum of 5, whereas their relative positions are reversed in the spectrum of 1 (Figure 4).

ROE Experiments of 1

A 2D ROESY (rotating-frame Overhauser effect spectroscopy)[24] spectrum of 1 was obtained at 700 MHz (Figure S1, Supporting Information). Key ROE cross-peaks were observed and confirmed stereochemical assignments. Specifically, ROE contacts were observed for (i) the C-19 cyclopropane *endo*/*exo* ring methylene protons, (ii) the proton network associated with the side chain configuration, and (iii) the presence of hydroxy groups at C-1 and C-15, which further defined the relative configuration of 1. The side chain signals associated with the three proton resonances of H-24, Me-26, and Me-27 were used as focal points for establishing the relative configuration. Proton H-24 exhibited ROE cross-peaks to H-23, Me-26, and Me-27. ROE cross-peaks were observed between H-23 and the neighboring protons H-22α, H-22β, H-17, and H-20. No correlations to H-15 were observed, which is consistent with the distances being >3.9 Å, as illustrated in the 3D model (Table 4 and Figure 5); a comprehensive analysis of ROE relationships in 1 are depicted in Figure 5.

Me-27 exhibited an ROE correlation to protons H-24, H-22α, and H-22β. To confirm the 23R,24R-type structural arrangement, the ROESY spectrum for 4 was also analyzed and compared in terms of the side chain system. Compound 4 showed an ROE correlation between H-24 and H-22α. An additional observed cross-peak was not clearly assignable due to extensive cross-peak overlap, but could represent the ROE correlation between the proton pairs H-24/H-17 and/or H-24/ H-26 and/or H-24/H-27. The important discriminating ROE correlations for establishing the configuration of the side chain were Me-27 to H-22α and H-22β, which is present only in a 23R,24R arrangement, and H-24 to H-22α, which is present only in a 23R,24S arrangement, respectively.

Structure Elucidation of Compound 2

3-O-α-L-Arabinopyranosyl-(1*S*,24*R*)-1,24,25-trihydroxy-15-oxo-acta-(16R,23R)-16,23-monoxoside (2) was isolated as a colorless film. The HRESIMS revealed a protonated molecule $[M + H]^+$ at *m/z* 637.3939 (calcd for $C_{35}H_{57}O_{10}$, 637.3952), indicating a molecular formula of $C_{35}H_{56}O_{10}$. The ^{1}H NMR spectrum displayed resonances associated with a cyclopropane methylene at δ 0.416 and 0.689 ppm, six tertiary methyls at δ 1.070, 1.173, 1.252, 1.375, 1.589, and 1.646 ppm, a secondary methyl at δ 0.959 ppm, and an anomeric proton at δ 4.813 ppm (d, J = 7.2 Hz; Figure S5, Supporting Information). Carbon chemical shifts were assigned from the HSQC experiment (Figure S8, Supporting Information) and confirmed the relative configurations of the D/E rings and side chain. The sugar moiety present in 2 was determined to be α-ara*p*, as the ^{13}C NMR resonances and ^{1}H NMR sugar spin–spin coupling patterns matched those of the previously isolated 3. HiFSA revealed that visual interpretation under first-order assumptions would ordinarily have overlooked discrete couplings. For example, while the H-4′ signal resembles a broad singlet on the acquired spectrum, it is dificult to resolve its multiplicity and extract all coupling constants visually. However, the HiFSA method led to deconvolution of the multiplicity as a ddd with J values of 1.61, 2.91, and 3.52 Hz. In the same manner as for 1, the signal for H-1 at δ 3.777 ppm was consistent with the presence of a hydroxy group at C-1.

Two HMBC cross-peaks (δ 3.891 ppm/214.5 and 1.187 ppm/214.5 ppm) indicated an isolated carbonyl group at C-15, consistent with a carbonyl group in a five-membered ring.[25] The gCOSY spectrum showed spin–spin coupling systems consistent with the proposed carbon framework. Thus, the structure of 2 was deduced as 3-O-α-L-arabinopyranosyl-(1*S*,24*R*)-1,24,25-trihydroxy-15-oxo-acta-(16R,23R)-16,23-monoxoside. Key HMBC correlations, consistent with the structure of 2, are depicted in Figure 6.

Other Triterpenes in the Aerial Parts of *A. racemosa*

In addition to the new compounds **1** and **2**, the following previously described triterpenes were isolated and characterized by a combination of MS and NMR methods (for complete ^{1}H NMR data, see Figures S9–15, Supporting Information): the binoxosides **3, 4, 6,** and **7**; the monoxoside **8**; and the binoxols **5** and **9**. The relative configurations of the glycosidic moieties were determined by ^{1}H,^{1}H spin–spin coupling analysis, as previously described. All of the compounds were isolated as colorless films, and estimation of their chemical purity by the 100% qHNMR method[26] led to the conclusion that their optical purities are insuficient to justify optical rotation measurements. This is supported by other

recent findings: even repeatedly purified *Actaea* triterpenes frequently contain several impurities that are distinctly different in structure, in particular regarding the stereogenic rings E and F;[12] the use of 2D NMR barcoding[27] enables both the distinction of components in residually complex mixtures and also shows the presence of minor impurities. As demonstrated for (12R)-12-acetoxy-(24*S*,25*R*)-24,25-epoxy-(26*R* and *S*)-26,27-dihydroxy-3-O-β-D-xylopyranosylacta-(16*S*,23*R*)-16,23;23,26-bi-noxoside,[27] differential HSQC analysis can identify new compounds as minor impurities in consecutive fractions that are residually complex.[12]

Two of the binoxosides, 3 and 4, share the same aglycone structure. A broad singlet for proton H-1 was observed at 3.824 and 3.836 ppm, respectively, suggesting the presence of a hydroxy group at position C-1 of the triterpene skeleton. For the side chain determination, a characteristic singlet (at 3.774 ppm for both 3 and 4) and a doublet (at 4.767 and 4.769 ppm with J = 9.2 Hz) were used to determine that these compounds are acta-(16S,23R, 24S)-16,23;16,24-binoxoside type, unlike the acta-(16*S*,23*R*,24*R*)-16,23;16,24-binoxoside type. The ^{1}H NMR chemical shifts agreed with those previously reported for 3[28] and 4.[17]

In a previous report on *A. simplex*,[8] OH 7β-derivatives of *Actaea* triterpenes have been identified only from aerial parts. Similarly, two OH 7β-derivatives, **5** and **6**, were now isolated from the aerial parts of *A. racemosa*; however, they have not been previously reported from its roots/rhizomes. The presence of a ^{1}H NMR pseudotriplet at 3.711 ppm for 5 and at 3.698 ppm for 6 suggested the occurrence of an OH group at C-7, which showed clear coupling correlations with H-6α, H-6β, and H-8 in the COSY spectrum (data not shown). For 6, an acetoxy methyl signal at 1.956 ppm was observed. Other proton signals were congruent with previously reported values.[28,29] (7S,15R)-7,15,25-Trihydroxy-acta-(16*S*,23*R*,24*S*)-16,23;16,24-binoxol (**5**) was isolated for the first time from a natural source in the form of an aglycone, although it has previously been obtained by enzymatic hydrolysis.[21]

The structures of compounds **7**–**9** were identified in a similar manner, and their spectroscopic data compared with previous values as follows. The structure of 7 was deduced, as its ^{1}H NMR assignments were consistent with previously reported NMR data.[30,31] This compound has been isolated from the roots/rhizomes of *A. racemosa*[32] and C. acerina[33] and also from the aerial parts of C. simplex[34] and C. dahurica.[35] Compound 8 was first isolated from *C. japonica* in 1981 by Sakurai et al.[36] and later from *C. racemosa*.[32] Subsequently, this compound has been isolated from *C. dahurica* and *A. rubra*.[37,38] Compound 9 has been previously isolated from the rhizomes of *C. dahurica* in 1975,[39] the rhizomes of *C. simplex* in 1977,[34] and the underground parts of *C. japonica* in 1981.[36] The earlier reports did not include full assignments of the ^{1}H NMR spectrum.

Identification of N_ω-Methylserotonin

The roots/ rhizomes of *A. racemosa* have been used widely to alleviate menopausal symptoms and were originally considered as an estrogenic agent (see ref 40 for a comprehensive review). Early clinical and in vivo studies suggested estrogen-like activity; however the majority of recent studies demonstrated a lack of estrogenic activity.[41–43] While this applies particularly for the major phytoconstituents, the cycloartane triterpenes

glycosides, they have been reported to possess antiproliferative activity against cancer cells[44,45] and antiosteoclastogenesis activity.[46] In terms of the alleviation of menopausal symptoms, a non-hormonal mechanism of action has been investigated instead of estrogenic activity. Consequently, serotonergic activity was revealed[47] and N_{ω}-methylserotonin (syn. N-methyl-5-hydroxytryptamine) identified as the compound responsible for such activity.[48] Although the main purpose of the present study was to investigate triterpenes representing the most abundant constituents of *Actaea* species, the presence of the serotonergic compound N_{ω}-methylserotonin was also examined to explore the phytochemical equivalence of the aerial parts compared to the roots/rhizomes. The quantity of N_{ω}-methylserotonin was analyzed in the methanolic extract of both aerial parts and roots/rhizomes of *A. racemosa* by LC-MSMS in SRM mode and determined to be 75 ppm w/w in the extract of the aerial parts, which was comparable to the 91 ppm w/w level contained in the extract of the roots/rhizomes. It should be noted that the levels obtained from this methanol extract are 3 times those reported in the initial discovery of N_{ω}-methylserotonin in the 75% ethanolic extract.[48]

CONCLUSION

The isolation and characterization of two new cycloartane compounds, **1** and **2**, along with seven previously known triterpenes (**3**–**9**), demonstrates that both similarities and distinctive characteristics exist in the triterpene glycoside portion of the *A. racemosa* metabolome of its aerial vs nonaerial plant parts. Among the seven known compounds, five (3–6, 9) were isolated from *A. racemosa* for the first time. They have been isolated from other *Actaea*/*Cimicifuga* species or obtained by enzymatic hydrolysis, but have not been isolated previously from the roots/rhizomes of *A. racemosa*. Thus, it is likely that they represent characteristic marker compounds of the aerial parts, and these plant parts have unique constituents.

Concerning the use of black cohosh preparations for women's health, N_{ω}-methylserotonin,[48,49] the cimicifugic acids, and the triterpenes are considered to be among the bioactive markers for *A. racemosa*. However, it is still unclear as to what the main active compounds are in terms of the clinical applications of the plant. Currently, *A. racemosa* extracts are standardized to their triterpene glycoside content, calculated as 23-*epi*-26-deoxyactein [(12*R*)-12-acetoxy-(24*R*,25*R*)-24,25-epoxy-3-O-β-D-xylopyranosylacta-(16*S*, 23*S*)-16,23;23,26-bi-noxoside]. In terms of triterpene glycosides, the aerial parts have the potential to serve as an alternative source to the roots/ rhizomes, because all of the isolated compounds in this study are clearly *A. racemosa*-characteristic cycloartane triterpenes. The serotonergic compound N_{ω}-methylserotonin was confirmed as being present in the aerial parts of *A. racemosa* as well. Although the quantity in the above-ground parts (75 ppm w/w in the extract) was slightly lower than in the roots/rhizomes (91 ppm *w/w* in the extract), the findings suggest that the aerial parts also exhibit at least some chemical equivalence to the roots/rhizomes of *A. racemosa* in terms of both serotonergic activity and possibly the content of other alkaloids known to occur in *Actaea*.[50]

The extensive structural analysis conducted on both new compounds, **1** and **2**, used various NMR techniques. Even though *A. racemosa* represents one of the most intensively studied

medicinal plants to date, this is the first report of fully matched simulated and experimental NMR spectra for the characterization of triterpene glycosides. Use of the HiFSA method established unambiguously the stereochemical relationships of the compounds and enabled their future rapid dereplication as well as their HiFSA-based quantitation in mixtures by NMR (HiFSA-qHNMR).[13,51] HiFSA also allowed for the identification of small but characteristic long-range (^{4}J) couplings that are "hidden" in some of the cycloartane triterpene peaks and previously have been reported as simple singlets or doublets.

Detailed analysis of the spin–spin coupling patterns in the xyl*p* and arap structural units in **1** and **2** provides a blueprint for the future rapid identification of these sugar moieties that occur commonly in *Actaea* triterpenes. The assignment of the two pentoses to their respective D-and L-series was based on the closely matching ^{13}C NMR resonances relative to corresponding resonance in previously investigated triterpenes, for which X-ray crystallographic reference structures with absolute stereochemical assignments exist.[52] This assignment is based on the theory that the diastereotopic dispersion of enantiomeric sugar moieties results in noticeable SCS effects in both the sugar and the A ring of the triterpene portions of the molecules. Similar considerations apply for the absolute stereochemistry of the aglycones. However, definitive assignments would require X-ray crystallographic analysis, which was precluded at this time by the lack of crystallinity of the low-yield isolates **1** and **2**.

EXPERIMENTAL SECTION

General Experimental Procedures

NMR experiments were performed on the following NMR spectrometers: a Bruker AVANCE-400 equipped with a room-temperature 5 mm BBO autotune probe, a Bruker AVANCE-600 and/or a Bruker AVANCE-900 equipped with 5 mm TXI and TCI autotune cryoprobe, respectively, and a Bruker AVANCE-700 equipped with a 1.7 mm TXI cryoprobe. All NMR experiments were acquired nonspinning with the temperature thermostatically controlled at 25 °C (298 K). The ^{1}H chemical shifts for all 1D ^{1}H and 2D homonuclear ^{1}H COSY spectra are expressed in parts per million (δ ppm) referenced to the residual protonated solvent signal (pyridine-d_4) at δ 7.217 ppm. For the 2D heteronuclear correlation data (HSQC and HMBC), spectra are expressed in parts per million (δ ppm) referenced to the pyridine-d_5 solvent resonances at δ 7.217 ppm in F2 (^{1}H) and δ 123.5 ppm in F1 (^{13}C). Offine FID processing was conducted with the Bruker TopSpin software. All 1D ^{1}H NMR spectra were routinely processed with a Lorentzian–Gaussian window function (LB = −1.0 and GB = 0.1) and zero-filled to 256 K points prior to Fourier transformation. The HiFSA calculations were performed using PERCH NMR spin simulation software (v. 2010.1, PERCH Solutions, Ltd., Kuopio, Finland). The 3D models were constructed using Chem 3D Pro (v. 11.0), and the structures were energy minimized using the MM2 module. Exact mass measurements and molecular formulas were obtained from LC-HRESIMS using a Waters SYNAPT quadrupole/time-of-fight spectrometer. Semipreparative RP-HPLC was carried out with a YMC-ODS semipreparative column (10 × 250 mm, 5 μm) on a Waters 600 Delta system with a CH_3CN (A)–H_2O (B) solvent system. Gradient conditions were 30% to 40% A in 30 min and 40% to 60% A in the following 40 min at a flow rate of 4 mL/

min. Fraction monitoring was by thin-layer chromatography (TLC) on precoated Alugram SIL G/UV silica gel 60 aluminum plates (0.20 mm) with a UV254 fluorescent indicator (10 × 20 cm; Macherey-Nagel, Düren, Germany). TLC fractions were visualized under UV light (254 and 365 nm) and then after spraying of the plates with a solution using vanillin/H_2SO_4 (general purpose reagent). HSCCC separations were conducted on a CCC-1000 J-type three-coiled planetary motion HSCCC (Pharma-Tech Research Corp., Baltimore, MD, USA), with a total volume of 320 mL using 3 × 107 mL PTFE Teflon tubing coils of 1.6 mm i.d., 2.6 mm o.d. CPC separations were performed on a Kromaton FCPC instrument with a 1 L (true volume 943 mL) and 200 mL (true volume 195 mL) rotors, with 1/16 in. connections. For HSCCC/CPC, the HEMWat, ChMWat, and HTerMWat solvent families were employed.[53]

Plant Material

Actaea racemosa was collected in Sevier County, Tennessee, USA. The plants were collected at an elevation of 3500 ft (June 1999) and identified by Dr. G. Ramsey, Department of Biology, Lynchburg College, Lynchburg, Virginia, USA. Voucher specimens have been deposited at the Ramsey-Freer Herbarium at Lynchburg College and at the Field Museum of Natural History Herbarium, Chicago, Illinois. Sequential extraction was carried out on 298 g of dried and milled plant material by the percolation method. To cover a wide polarity range, the following three different solvents were used: petroleum ether, dichloromethane (CH_2Cl_2), and 75% EtOH. The dried residues from the three solvent extractions were combined in aliquots that were proportional to the yield of each of the individual extracts to produce a 20 g sample of total extract. This combined extract was partitioned in a separatory funnel in a solvent system consisting of hexanes, EtOAc, MeOH, and water (1:9:1:9) (HEMWat +7; partitioning five times, with 400 mL each) to provide 3.2 g of upper phase-soluble partition and 16.0 g of lower phase-soluble partition. Insoluble material (0.3 g) was obtained from the boundary area between the upper and lower phase.

Extraction and Isolation

The lower phase of the partition (16 g) was chromatographed on a normal-phase silica gel vacuum liquid chromatography (VLC) (240 g) with a gradient of increasing polarity of a solvent system consisting of Hex to EtOAc, then EtOAc to MeOH, and finally MeOH to H_2O, to yield 62 fractions. Fractions 19–27, which eluted using a gradient from a mixture of hexanes– EtOAc (90%) to a mixture of EtOAc–MeOH (30%), were combined based on their TLC profiles and fractionated further by centrifugal partition chromatography (CPC) (200 mL rotor, S_f = 0.67, flow rate 4 mL/min) into six subfractions using the ChMWat 0 solvent system ($CHCl_3$–MeOH–H_2O, 10:3:7), with the upper phase as a mobile phase. Preparative HPLC of CPC subfraction **4**, which eluted between K = 0.5 and 1.0, was carried out as the next step. Two new compounds were obtained, (1*S*,15*R*)-1,15,25-trihydroxy-3-O-*β*-D-xylopyranosyl-acta-(16*S*,23*R*,24*R*)-16,23;16,24-binoxoside (**1**) (0.37 mg), eluted at a retention time of 41 to 44 min, and 3-O-*α*-L-arabinopyranosyl-(1*S*,24*R*)-1,24,25-trihydroxy-15-oxo-acta-(16R,23R)-16,23-monoxo-side (**2**) (4.00 mg), at a retention time of 62 min, together with the known compounds 3 (0.87 mg), at a retention time of 54 to 58 min, and 4 (0.18 mg), at a retention time of 66 min.

VLC fractions 11–16, which were subjected to gradient elution with a mixture of 50% hexanes and 50% EtOAc to a mixture of 25% hexanes and 75% EtOAc, were further chromatographed by normalphase VLC using a solvent gradient of petroleum ether–$CHCl_3$–MeOH (5:9:1) to $CHCl_3$–MeOH (9:1), to MeOH, to yield 44 subfractions. Subtractions 6–10, which eluted with petroleum ether–$CHCl_3$–MeOH (5:9:1) after about one column volume, were combined according to their TLC profiles. Preparative HPLC of the combined fraction used the previously described conditions and yielded 5 (0.13 mg), at a retention time of 43 min, and that of subfractions of 11–13 yielded 6 (0.25 mg), at a retention time of 26 min, 7 (6.19 mg), at a retention time of 43 min, and 8 (1.11 mg), at a retention time of 54 min. The upper phase partition (3.2 g) was subjected to CPC (200 mL rotor) using the ChMWat 0 solvent system ($CHCl_3$–MeOH–H_2O, 10:3:3), with the upper phase used as mobile phase, to yield four combined fractions (S_f = 0.78; flow rate 4 mL/ min). CPC fraction 2 (311.9 mg, eluting between K = 0.2 and 2.0) was fractionated further by 320 mL of HSCCC (S_f = 0.88; flow rate 1.5 mL/min) with an orthogonal solvent system using the upper phase as a mobile phase. The orthogonal system was HTerMWat (hexanes– *tert*-butyl methyl ether–MeOH–H_2O), a variation of the HEMWat family that uses tBME instead of EtOAc. Nine combined fractions were obtained from this fractionation, and subfractions 1–5 (K = 0.2– 1.0) were combined on the basis of their TLC profiles. The combined subfraction was then subjected to 125 mL of HSCCC with HEMWat-4 (hexanes–EtOAc–MeOH–H_2O, 7:3:6:4), using the upper phase as a mobile phase, to yield 9 (0.97 mg) at about K = 1.

(1*S*,15*R*)-1,15,25-Trihydroxy-3-O-β-D-xylopyranosyl-acta-(16*S*,23*R*,24*R*)-16,23;16,24-binoxoside (1): colorless film; NMR (900 MHz, C_5D_5N) see Table 3; HRESIMS *m/z* 659.3743 $[M + Na]^+$, calcd for $C_{35}H_{56}O_{10}Na$ (–4.2 ppm), 659.3771.

3-O-α-L-Arabinopyranosyl-(1*S*,24*R*)-1,24,25-trihydroxy-15-oxo-acta-(16R,23R)-16,23-monoxoside (2): colorless film; NMR (900 MHz, C_5D_5N) see Table 5; HRESIMS *m/z* 637.3939 $[M + H]^+$, calcd for $C_{35}H_{57}O_{10}$ (–2.0 ppm), 637.3952.

3-O-α-L-Arabinopyranosyl-(1*S*,15*R*)-1,15,25-trihydroxy-acta-(16S,23R,24S)-16,23;16,24-binoxoside (3): colorless film; ^1H NMR (900 MHz, C_5D_5N) aglycone moiety δ 4.767 (1H, brd, J = 9.2 Hz, H-23), 4.480 (1H, brd, 7.6 Hz), 4.353 (1H, dd, J = 4.5, 12.0 Hz, H-3), 4.312 (1H, d, J = 7.6 Hz, H-15), 3.824 (1H, brs, H-1), 3.774 (1H, s, H-24), 2.879 (1H, m, H-11α), 2.754 (1H, ddd, J = 13.3, 4.1, 4.1 Hz, H-2α), 2.475 (1H, dd, J = 4.7, 12.6 Hz, H-5), 2.281 (1H, overlapped, H-22β), 2.258 (1H, overlapped, H-2β), 2.159 (1H, m, H-7α), 1.788 (1H, overlapped, H-12β), 1.766 (1H, dd, J = 3.8, 12.5 Hz, H-8), 1.686 (1H, m, H-20), 1.667 (1H, overlapped, H-6α), 1.627 (1H, overlapped, H-12α), 1.513 (1H, d, J = 14.8, H-17), 1.495 (3H, s, H-27),[54] 1.477 (3H, s, H-26),[54] 1.414 (1H, m, 11β), 1.384 (1H, overlapped, H-7β), 1.377 (3H, s, H-29), 1.275 (3H, s, H-28), 1.207 (3H, s, H-18), 1.096 (3H, s, H-30), 1.026 (1H, dt, J = 1.8, 11.9 Hz, H-22α), 0.854 (3H, d, J = 6.5 Hz, H-21), 0.852 (1H, m, H-6β), 0.707 (1H, d, J = 4.2 Hz, H-19 *endo*), 0.431 (1H, d, J = 4.2 Hz, H-19 *exo*); sugar moiety δ 4.820 (1H, d, J = 7.1 Hz, H-1′), 4.465 (1H, dd, J = 7.1, 8.1 Hz, H-2′), 4.139 (1H, dd, J = 3.5, 8.8 Hz, H-3′), 4.291 (1H, m, H-4′), 4.212 (1H, dd, J = 12.2, 2.9 Hz, H-5′α), 3.658 (1H, dd, J = 12.2, 1.1 Hz, H-5′β); HRESIMS *m/z* 659.3777 $[M + Na]^+$, calcd for $C_{35}H_{56}O_{10}Na$ (0.9 ppm), 559.3771.

(1*S*,15*R*)-1,15,25-Trihydroxy-3-O-*β*-D-xylopyranosyl-acta-(16S,23R,24S)-16,23;16,24-binoxoside (4): colorless film; ^{1}H NMR (900 MHz, C_5D_5N) aglycone moiety *δ* 4.769 (1H, d, *J* = 9.2 Hz, H-23), 4.483 (1H, d, *J* = 8.7 Hz, OH-15), 4.374 (1H, dd, *J* = 4.5, 12.1 Hz, H-3), 4.312 (1H, d, *J* = 8.7 Hz, H-15), 3.836 (1H, brs, H-1), 3.774 (1H, s, H-24), 2.884 (1H, m, H-11*α*), 2.749 (1H, ddd, *J* = 13.3, 4.1, 4.1 Hz, H-2*α*), 2.489 (1H, dd, *J* = 4.7, 12.7, H-5), 2.281 (1H, overlapped, H-22*α*), 2.272 (1H, overlapped, H-2*β*), 2.162 (1H, m, H-7*α*), 1.787 (1H, overlapped, H-12*α*), 1.769 (1H, dd, *J* = 4.2, 12.4 Hz, H-8), 1.687 (1H, overlapped, H-6*α*), 1.678 (1H, overlapped, H-20), 1.632 (1H, m, H-12*β*), 1.501 (3H, s, H-27),[54] 1.495 (1H, overlapped, H-17), 1.480 (3H, s, H-26),[54] 1.426 (1H, overlapped, H-11*β*), 1.420 (3H, s, H-29), 1.388 (1H, m, H-7*β*), 1.273 (3H, s, H-28), 1.206 (3H, s, H-18), 1.135 (3H, s, H-30), 1.026 (1H, dt, *J* = 1.8, 11.9 Hz, H-22*β*), 0.861 (1H, overlapped, H-6*β*), 0.853 (3H, d, *J* = 6.2 Hz, H-21), 0.714 (1H, d, *J* = 4.2 Hz, H-19 endo), 0.437 (1H, d, *J* = 4.2 Hz, H-19 *exo*); sugar moiety *δ* 4.890 (1H, d, *J* = 7.6 Hz, H-1′), 4.249 (1H, dd, *J* = 5.0, 11.0 Hz, H-5′*β*), 4.223 (1H, m, H-4′), 4.133 (1H, t, *J* = 8.8 Hz, H-3′), 4.052 (1H, m, H-2′), 3.586 (1H, t, *J* = 10.5 Hz, 5′*α*); HRESIMS *m/z* 637.3958 $[M + H]^+$, calcd for $C_{35}H_{57}O_{10}$ (0.9 ppm), 637.3952.

(7S,15R)-7,15,25-Trihydroxy-acta-(16S,23R,24S)-16,23;16,24-bi-noxol (5): colorless film; ^{1}H NMR (900 MHz, C_5D_5N) *δ* 6.511 (1H, d, *J* = 6.5 Hz, OH-15), 4.800 (1H, d, *J* = 9.2 Hz, H-23), 4.485 (1H, d, *J* = 6.5 Hz, H-15), 3.802 (1H, s, H-24), 3.711 (1H, brt, *J* = 10.7 Hz, H-7), 3.577 (1H, ddd, *J* = 11.2, 4.5, 4.5 Hz, H-3), 2.301 (1H, m, H-22*β*), 2.110 (1H, m, H-11a), 2.085 (1H, ddd, *J* = 12.6, 3.7, 3.7 Hz, H-6a), 2.017 (1H, m, H-2*α*),1.909 (1H, m, H-2*β*), 1.846 (1H, d, *J* = 10.7 Hz, H-8), 1.711 (1H, overlapped, H-12a), 1.695 (1H, overlapped, H-20), 1.605 (1H, overlapped, H-12b), 1.600 (1H, overlapped, H-5), 1.586 (1H, overlapped, H-1a), 1.566 (1H, d, *J* = 11.0 Hz, H-17), 1.534 (3H, s, H-26),[54] 1.513 (3H, s, H-27),[54] 1.324 (3H, s, H-28), 1.253 (1H, overlapped, H-6b), 1.246 (3H, s, H-29), 1.237 (1H, overlapped, H-1b), 1.223 (3H, s, H-18), 1.132 (3H, s, H-30), 1.110 (1H, m, H-11b), 1.065 (1H, dt, *J* = 1.8, 11.9 Hz, H-22*α*), 0.894 (3H, s, H-21), 0.731 (1H, d, *J* = 4.3 Hz, H-19 endo), 0.414 (1H, d, *J* = 4.3 Hz, H-19 *exo*); HRESIMS *m/z* 505.3512 $[M + H]^+$, calcd for $C_{30}H_{49}O_6$ (–3.4 ppm), 505.3526.

25-Acetoxy-(7S,15R)-7,15-dihydroxy-3-O-*β*-D-xylopyranosyl-acta-(16S,23R, 24S)-16,23;16,24-binoxoside (6): colorless film; ^{1}H NMR (900 MHz, C_5D_5N) aglycone moiety *δ* 4.616 (1H, d, *J* = 9.2 Hz, H-23), 4.458 (1H, d, *J* = 6.8 Hz, H-15), 4.167 (1H, s, H-24), 3.698 (1H, brt, *J* = 10.7 Hz, H-7), 3.542 (1H, dd, *J* = 11.2, 4.3 Hz, H-3), 2.390 (1H, m, H-2*β*), 2.281 (1H, m, H-22*β*), 2.072 (1H, m, H-11a), 2.039 (1H, m, H-6a), 1.964 (1H, overlapped, H-2*α*), 1.956 (3H, s, 25-OAc), 1.817 (1H, d, *J* = 10.2, H-8), 1.739 (3H, s, H-27), 1.731 (3H, s, H-26), 1.677 (1H, overlapped, H-12a), 1.667 (1H, overlapped, H-20), 1.618 (1H, overlapped, H-5), 1.605 (1H, overlapped, H-1a), 1.581 (1H, overlapped, H-12b), 1.516 (1H, d, *J* = 10.9 Hz, H-17), 1.360 (3H, s, H-29), 1.299 (3H, s, H-28), 1.241 (1H, m, H-1b), 1.189 (3H, s, H-18), 1.187 (1H, overlapped, H-6b), 1.087 (3H, s, H-30), 1.063 (1H, overlapped, H-11b), 1.016 (1H, overlapped, H-22*α*), 0.874 (3H, d, *J* = 6.6 Hz, H-21), 0.679 (1H, d, *J* = 4.3 Hz, H-19 endo), 0.361 (1H, d, *J* = 4.3 Hz, H-19 *exo*); sugar moiety *δ* 4.879 (1H, d, *J* = 7.5 Hz, H-1′), 4.382 (1H, brt, *J* = 10.8, 10.8 Hz, H-5′*β*), 4.257 (1H, m, H-4′), 4.181 (1H, overlapped, H-3′), 4.056 (1H, m, H-2′), 3.753 (1H, dd, *J* = 5.2, 11.4 Hz, H-5′*α*); HRESIMS *m/z* 679.4030 $[M + H]^+$, calcd for $C_{37}H_{59}O_{11}$ (4.0 ppm), 679.4057.

25-Acetoxy-(15R)-15-hydroxy-3-O-β-D-xylopyranosylacta-(16S,23R,24S)-16,23;16,24-binoxoside (7): colorless film; ^{1}H NMR (900 MHz, C_5D_5N) aglycone moiety δ4.603 (1H, d, *J* = 9.2 Hz, H-23), 4.280 (1H, d, *J* = 9.2 Hz, H-15), 4.123 (1H, s, H-24), 3.532 (1H, dd, *J* = 4.3, 11.8 Hz, H-3), 2.386 (1H, m, H-2α), 2.267 (1H, m, H-22β), 2.128 (1H, m, H-7a), 2.086 (1H, m, H-11a), 1.975 (1H, overlapped, H-2β), 1.975 (3H, s, 25-OAc), 1.706 (1H, overlapped, H-8), 1.695 (3H, s, H-26), 1.680 (1H, overlapped, H-12a), 1.674 (3H, s, H-27), 1.660 (1H, overlapped, H-20), 1.615 (1H, m, 1α), 1.553 (1H, overlapped, H-12b), 1.542 (1H, overlapped, H-6α), 1.465 (1H, d, *J* = 11.1 Hz, H-17), 1.353 (1H, overlapped, H-5), 1.331 (3H, s, H-29), 1.250 (1H, m, 1β), 1.202 (3H, s, H-28), 1.190 (1H, overlapped, H-7b), 1.153 (3H, s, H-18), 1.078 (1H, overlapped, H-11), 1.071 (3H, s, H-30), 0.987 (1H, dt, *J* = 1.8, 11.8 Hz, H-22α), 0.853 (3H, d, *J* = 6.5 Hz, H-21), 0.730 (1H, m, H-6α), 0.537 (1H, d, *J* = 4.2 Hz, H-19 *endo*), 0.299 (1H d, *J* = 4.2 Hz, H-19 *exo*); Sugar moiety δ4.879 (1H, d, *J* = 7.5 Hz, H-1′), 4.376 (1H, dd, *J* = 5.3, 11.4 Hz, H-5′β), 4.245 (1H, m, H-4′), 4.179 (1H, t, *J* = 8.8 Hz, H-3′), 4.055 (1H, m, H-2′), 3.755 (1H, t, *J* = 11.0 Hz, H-5′α); HRESIMS *m/z* 663.4092 $[M + H]^+$, calcd for $C_{37}H_{59}O_{10}$ (–2.4 ppm), 663.4108.

(24S)-24-Acetoxy-(15R,16R)-15,16,25-trihydroxy-3-O-β-D-xylopyr-anosyl-acta-(23S)-16,23-monoxoside (8): colorless film; ^{1}H NMR (900 MHz, C_5D_5N) aglycone moiety δ5.785 (1H, d, *J* = 8.5 Hz, H-24), 4.457 (1H, m, H-23), 4.166 (1H, d, *J* = 6.7 Hz, H-15), 3.533 (1H, dd, *J* = 11.8, 4.4 Hz, H-3), 2.389 (1H, m, H-2α), 2.133 (3H, s, 24-OAc), 2.079 (1H, overlapped, H-11a), 2.061 (1H, overlapped, H-7a), 2.054 (1H, overlapped, H-22a), 1.974 (1H, m, H-2β), 1.843 (1H, d, *J* = 10.0 Hz, H-17), 1.830 (1H, overlapped, H-22b), 1.791 (1H, dd, *J* = 12.4, 5.0 Hz, H-8), 1.778 (1H, m, H-20), 1.716 (1H, m, H-12a), 1.619 (1H, overlapped, H-1a), 1.600 (1H, overlapped, H-6α), 1.557 (1H, m, H-12b), 1.522 (3H, s, H-26), 1.488 (3H, s, H-27), 1.369 (1H, dd, *J* = 4.1, 12.4 Hz, H-5), 1.333 (3H, s, H-29), 1.288 (1H, m, H-1β), 1.257 (1H, m, H-7b), 1.246 (3H, s, H-18), 1.235 (3H, s, H-28), 1.111 (1H, m, H-11b), 1.055 (3H, s, H-30), 0.974 (3H,d, *J* = 6.5 Hz, H-21), 0.791 (1H, m, 6β), 0.565 (1H, d, *J* = 3.9 Hz, H-19 endo), 0.292 (1H, d, *J* = 3.9 Hz, H-19 *exo*); sugar moiety δ4.901 (1H, d, *J* = 7.6 Hz, H-1′), 4.403 (1H, dd, 5.0, 11.2 Hz, H-5′β), 4.264 (1H, m, H-4′), 4.198 (1H, t, *J* = 8.9 Hz, H-3′), 4.068 (1H, m, H-2′), 3.789 (1H, dd, *J* = 10.8 Hz, H-5′α); HRESIMS *m/z* 703.4036 $[M + Na]^+$, calcd for $C_{37}H_{60}O_{11}Na$ (0.4 ppm), 703.4033.

(15R)-15,25-Dihydroxy-acta-(16S,23R,24S)-16,23;16,24-binoxol (9): colorless film; ^{1}H NMR (900 MHz, C_5D_5N) δ4.789 (1H, brd, *J* = 8.9 Hz, H-23), 4.340 (1H, s, H-15), 3.804 (1H, s, H-24), 3.569 (1H, dd, *J* = 4.6, 11.6 Hz, H-3), 2.299 (1H, m, H-22β) 2.136 (2H, overlapped, H-11a and H-7a), 2.020 (1H, m, H-2α), 1.923 (1H, m, H-2β), 1.737 (1H, dd, *J* = 4.5, 12.6 Hz, H-8), 1.698 (1H, m, overlapped, H-20), 1.610 (1H, overlapped, H-1a), 1.585 (1H, overlapped, H-7a), 1.5312 (1H, d, *J* = 11.0, H-17), 1.522 (3H, s, H-26), 1.500 (3H, s, H-27), 1.335 (1H, overlapped, H-6α), 1.324 (3H, s, H-27), 1.240 (1H, overlapped, H-1b), 1.228 (3H, s, H-29), 1.219 (3H, s, H-28), 1.195 (3H, s, H-18), 1.134 (1H, overlapped, H-7b), 1.117 (1H, s, H-30), 1.055 (1H, m, H-22α), 0.881 (1H, d, *J* = 6.6 Hz, H-21), 0.796 (1H, m, H-6β), 0.593 (1H, d, *J* = 4.2 Hz, H-19 endo), 0.351 (1H, d, *J* = 4.2 Hz, 19 *exo*); HRESIMS *m/z* 511.3381 $[M + Na]^+$, calcd for $C_{30}H_{48}O_5Na$ (–3.9 ppm), 511.3399.

Note: *When the configuration of the methylene hydrogens could be clearly identified from the NMR spectrum, the α and β notations were assigned. Otherwise, the methylene protons

are arbitrarily described as a and b, in the order of their chemical shifts, starting from lower field.

Quantitative Analysis of N_{ω}-Methylserotonin

The analyses were carried out using an Agilent 1200 HPLC system interfaced to an Agilent 6410 triple quadruple mass spectrometer. The analytes were separated on an Agilent Zorbax Eclipse XDB C_{18} column (4.6 × 50 mm, 1.8 μm particle size) using an isocratic mobile phase of 8.5% MeOH in H_2O containing 0.1% formic acid. The flow rate was 300 μL/min, and the column temperature 25 °C. The retention times of N_{ω}-methylserotonin and serotonin were 4.8 and 4.3 min, respectively.

Positive-ion electrospray tandem mass spectrometry at unit resolution was used to measure N_{ω}-methylserotonin and serotonin with collision-induced dissociation and selected reaction monitoring (SRM). Nitrogen was used as a collision gas. During SRM, the analytes were measured by monitoring the transition of the protonated molecule of *m/z* 192 (N_{ω}-methylserotonin) and *m/z* 177 (serotonin) to the most abundant fragment ion of *m/z* 160. The SRM dwell time was 1 s/ion. The ion source parameters were as follows: capillary voltage, 4000 V; nebulizer gas pressure, 25 psi; fragmentor voltage, 95 V (N_{ω}-methylserotonin) and 70 V (serotonin); collision gas temperature, 300 °C; collision gas flow, 6 L/min; and collision energy, 3 eV (N_{ω}-methylserotonin) and 5 eV (serotonin). Data were acquired and analyzed using Agilent MassHunter Workstation software. Reference material was authenticated by qHNMR prior to use.

Supplementary Material

Refer to Web version on PubMed Central for supplementary material.

ACKNOWLEDGMENTS

We would like to acknowledge Dr. B. Ramirez for his assistance with the CSB NMR instrumentation. We are also very grateful to Mr. I. Burton, Dr. J. Walter, and Dr. T. Karakach, IMB/ NRC, Halifax, Canada, for their support and the acquisition of 700 MHz NMR data. Financial support for this research was provided by grant P50 AT000155 (UIC/NIH Botanical Center) from the National Center for Complementary and Alternative Medicine (NCCAM) and the Office of Dietary Supplements (ODS) of the National Institutes of Health (NIH). The construction of the UIC-CSB NMR facility and purchase of the 600 and 900 MHz NMR spectrometers were funded by NIHGMS grant P41 GM068944 awarded to Dr. P. G. W. Gettins.

REFERENCES

(1). Ankli A, Reich E, Steiner M. J. AOAC Int. 2008; 91:1257–1264. [PubMed: 19202784]

(2). Xie J, Wang C, Wang A, Wu J, Basila D, Yuan C. Acta Pharmacol. Sin. 2005; 26:1104–1110. [PubMed: 16115378]

(3). Attele AS, Zhou Y-P, Xie J-T, Wu JA, Zhang L, Dey L, Pugh W, Rue PA, Polonsky KS, Yuan C-S. Diabetes. 2002; 51:1851–1858. [PubMed: 12031973]

(4). Xie J-T, Mehendale SR, Wang A, Han AH, Wu JA, Osinski J, Yuan C-S. Pharmacol. Res. 2004; 49:113–117. [PubMed: 14643691]

(5). Wang C-Z, Zhang B, Song W-X, Wang A, Ni M, Luo X, Aung HH, Xie J-T, Tong R, He T-C. J. Agric. Food Chem. 2006; 54:9936–9942. [PubMed: 17177524]

(6). Imai, A. Pharmacognosy of the Aerial Parts of Black Cohosh (*Cimicifuga racemosa*). University of Illinois at Chicago; Chicago: 2013. Ph.D. Dissertation

(7). Crum JD, Cassady JM, Olmstead PM, Picha N. J. Proc. West Virginia Acad. Sci. 1965; 37:143–147.

(8). Kusano G. Yakugaku Zasshi. 2001121:497–521. [PubMed: 11494597]

(9). Liu Y, Chen DH, Si JY, Pan RL, Tu GZ, An DG. Yao Xue Xue Bao. 2003; 38:763–766. [PubMed: 14730900]

(10). Pan RL, Chen DH, Si JY, Zhao XH, Li Z, Cao L. Arch. Pharmacal Res. 2009; 32:185–190.

(11). Wang W-H, Nian Y, He Y-J, Wan L-S, Bao N-M, Zhu G-L, Wang F, Qiu M-H. Tetrahedron. 2015; 71:8018–8025.

(12). Qiu F, Imai A, McAlpine J, Lankin DC, Burton IW, Karakach TK, Farnsworth NR, Chen S-N, Pauli GF. J. Nat. Prod. 2012; 75:432–443. [PubMed: 22320430]

(13). Napolitano JG, Lankin DC, Graf TN, Friesen JB, Chen S-N, McAlpine JB, Oberlies NH, Pauli GF. J. Org. Chem. 2013; 78:2827–2839. [PubMed: 23461697]

(14). Napolitano JG, Lankin DC, Chen S-N, Pauli GF. Magn. Reson. Chem. 2012; 50:569–575. [PubMed: 22730238]

(15). Riihinen K, Mihaleva V, Gödecke T, Soininen P, Laatikainen R, Vervoort JM, Lankin DC, Pauli GF. Phytochem. Anal. 2013; 24:476–483. [PubMed: 23703898]

(16). Kusano A, Takahira M, Shibano M, Miyase T, Kusano G. Chem. Pharm. Bull. 1999; 47:511–516.

(17). Kusano A, Shimizu K, Idoji M, Shibano M, Minoura K, Kusano G. Chem. Pharm. Bull. 1995; 43:279–283.

(18). Bhacca NS, Gurst JE, Williams DH. J. Am. Chem. Soc. 1965; 87:302–305. [PubMed: 14228460]

(19). Williams DH, Bhacca NS. J. Am. Chem. Soc. 1963; 85:2861.

(20). Williamson KL, Howell T, Spencer TA. J. Am. Chem. Soc. 1966; 88:325–334.

(21). Williamson KL, Sloan LR, Howell T, Spencer TA. J. Org. Chem. 1966; 31:436–438.

(22). Williamson KL, Spencer TA. Tetrahedron Lett. 1965; 6:3267–3272.

(23). Bhacca, NS.; Williams, DH. Applications of NMR Spectroscopy in Organic Chemistry. Illustrations from the Steroid Field. Holden-Day, Inc.; San Francisco: 1964. p. 115-123.

(24). Bax A, Davis DAJ. Magn. Reson. 1985; 63:207–213.

(25). Shao Y, Harris A, Wang MF, Zhang HJ, Cordell GA, Bowman M, Lemmo E. J. Nat. Prod. 2000; 63:905–910. [PubMed: 10924163]

(26). Gödecke T, Napolitano JG, Rodriguez Brasco MF, Chen S-N, Jaki BU, Lankin DC, Pauli GF. Phytochem. Anal. 2013; 24:581–597. [PubMed: 23740625]

(27). Qiu F, McAlpine JB, Lankin DC, Burton I, Karakach T, Chen S-N, Pauli GF. Anal. Chem. 2014; 86:3964–3972. [PubMed: 24673652]

(28). Kusano G, Idoji M, Sogoh Y, Shibano M, Kusano A, Iwashita T. Chem. Pharm. Bull. 1994; 42:1106–1110.

(29). Kusano A, Shibano M, Kusano G. Chem. Pharm. Bull. 1995; 43:1167–1170.

(30). Kusano A, Shibano M, KItagawa S, Kusano G, Nozoe S, Fushiya S. Chem. Pharm. Bull. 1994; 42:1940–1943.

(31). Ye W, Zhang J, Che CT, Ye T, Zhao S. Planta Med. 1999; 65:770–772. [PubMed: 17260302]

(32). Chen S-N, Fabricant DS, Fong HHS, Farnsworth NR. J. Nat. Prod. 2002; 65:1391–1397. [PubMed: 12398533]

(33). Takemoto T, Kusano G, Yamamoto N. Yakugaku Zasshi. 1970; 90:68–72. [PubMed: 5462158]

(34). Kusano G, Hojo S, Kondo Y, Takemoto T. Chem. Pharm. Bull. 1977; 25:3182–3189.

(35). Liu Y, Chen D, Si J, Tu G, An D. J. Nat. Prod. 2002; 65:1486–1488. [PubMed: 12398548]

(36). Sakurai N, Kimura O, Inoue T, Nagai M. Chem. Pharm. Bull. 1981; 29:955–960.

(37). Ali Z, Khan SI, Khan IA. Planta Med. 2006; 72:1350–1352. [PubMed: 17024608]

(38). Kimura O, Sakurai N, Inoue T. Yakugaku Zasshi. 1983; 103:293–299. [PubMed: 6620129]

(39). Sakurai N, Nagai M, Inoue T. Yakugaku Zasshi. 1975; 92:724–728. [PubMed: 5066374]

(40). Qiu, F.; McAlpine, JB.; Krause, E.; Chen, S-N.; Pauli, GF. Progress in the Chemistry of Organic Natural Products. Kinghorn, AD.; Falk, H.; Kobayashi, J.-i., editors. Vol. 99. Springer; Vienna: 2014. p. 1-68.

(41). Betz JM, Anderson L, Avigan MI, Barnes J, Farnsworth NR, Gerden B, Henderson L, Kennelly EJ, Koetter U, Lessard S, Low Dog T, McLaughlin M, Naser B, Osmers RGW, Pellicore LS, Senior JR, van Breemen RB, Wuttke W, Cardellina JH II. Nutrition Today. 2009; 44:155–162.

(42). Mahady GB, Fabricant DS, Chadwick LR, Dietz B. Nutr. Clin. Care. 2002; 5:283–289. [PubMed: 12557811]

(43). Mahady GB. Nutr. Rev. 2003; 61:183–186. [PubMed: 12822708]

(44). Sun L-R, Qing C, Zhang Y-L, Jia S-Y, Li Z-R, Pei S-J, Qiu M-H, Gross ML, Qiu SX. Beilstein J. Org. Chem. 2007; 3:3. [PubMed: 17266751]

(45). Tian Z, Yang M, Huang F, Li K, Si J, Shi L, Chen S, Xiao P. Cancer Lett. 2005; 226:65–75. [PubMed: 16004933]

(46). Qiu SX, Dan C, Ding LS, Peng S, Chen S-N, Farnsworth NR, Nolta J, Gross ML, Zhou P. Chem. Biol. 2007; 14:860–869. [PubMed: 17656322]

(47). Burdette JE, Liu J, Chen S-N, Fabricant DS, Piersen CE, Barker EL, Pezzuto JM, Mesecar AD, van Breemen RB, Farnsworth NR, Bolton JL. J. Agric. Food Chem. 2003; 51:5661–5670. [PubMed: 12952416]

(48). Powell SL, Gödecke T, Nikolic D, Chen S-N, Dietz B, Farnsworth NR, van Breemen RB, Lankin DC, Pauli GF, Bolton JL. J. Agric. Food Chem. 2008; 56:11718–11726. [PubMed: 19049296]

(49). Gödecke T, Nikolic D, Lankin DC, Chen S-N, Powell SL, Dietz B, Bolton JL, van Breemen RB, Farnsworth NR, Pauli GF. Phytochem. Anal. 2009; 20:120–131. [PubMed: 19140115]

(50). Nikolić D, Gödecke T, Chen S-N, White J, Lankin DC, Pauli GF, van Breemen RB. Fitoterapia. 2012; 83:441–460. [PubMed: 22178683]

(51). Napolitano JG, Gödecke T, Lankin DC, Jaki BU, McAlpine JB, Chen S-N, Pauli GF. J. Pharm. Biomed. Anal. 2014; 93:59–67. [PubMed: 23870106]

(52). Chen S-N, Li W, Fabricant DS, Santarsiero BD, Mesecar AD, Fitzloff JF, Fong HHS, Farnsworth NR. J. Nat. Prod. 2002; 65:601–605. [PubMed: 11975513]

(53). Friesen JB, Pauli GFJ. Liq. Chromatogr. Relat. Technol. 2005; 28:2877–2806.

(54). The chemical shifts of the two Me groups attached to C-25 are conformationally averaged, via rotation along the C-24/C-25 bond. However, the nature of the resulting conformational populations has not been fully elucidated. Accordingly, the assignments of H-26 and H-27 for compound 3–9 were based on the ROE-based assignments made for **1** and **2** and, thus, are tentative for **3**–**9**

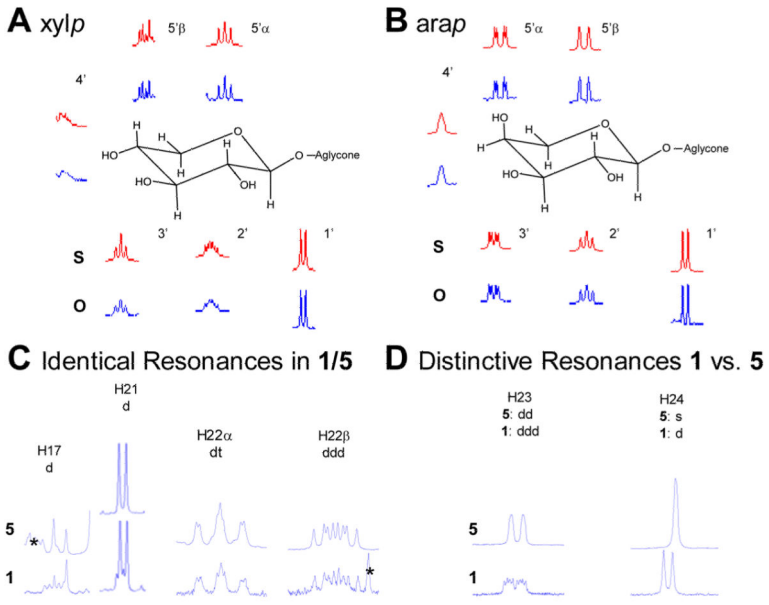

Figure 1.

HiFSA spin simulation analysis of typical saccharides (A, B) and the side chain substructure of **1** (C, D). HiFSA spin simulation of the ^{1}H NMR signals of the (A) β-D-xylopyranoside (xylp) spin system in **4** and (B) α-L-arabinopyranose (arap) spin system in **2**. Top signals (in red marked with "S") represent the simulated and the bottom signals (in blue marked with "O") the experimentally observed signals for **2**. (C, D) Comparison of the ^{1}H NMR signals for **1** (top) and **5** (bottom) in rings E and F, respectively. The signal for H-20 is not displayed, as it could not be analyzed due to extensive signal overlap. Signals marked with asterisks (*) belong to peaks of other spin systems.

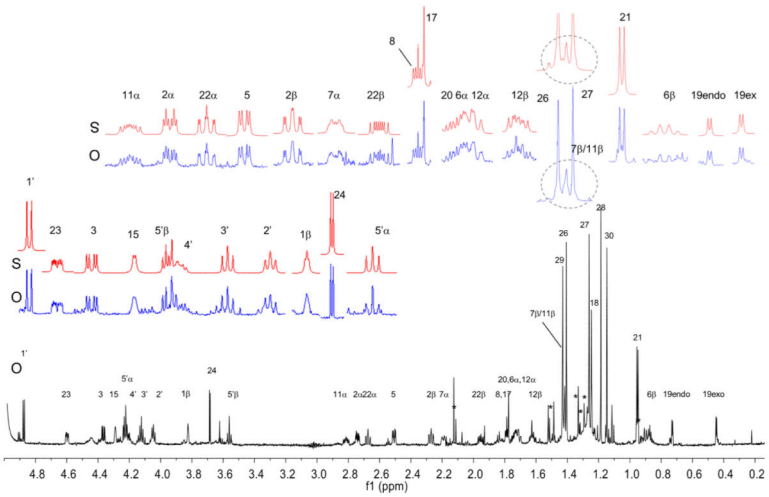

Figure 2.

^{1}H NMR spectrum (900 MHz) of 1 in pyridine-d_5. This sample contained 22–28% of an unidentified structurally related impurity, calculated from the signals of H-1′ (29%: 71%) and H-19-*endo* (22%:78%). Impurity peaks are denoted by *. Original spectra are denoted with an “O” (blue), and the corresponding HiFSA simulations are marked with an “S” (red).

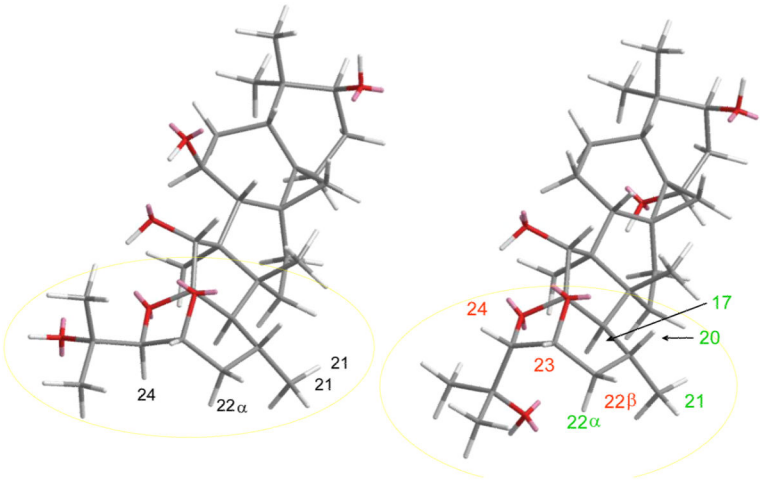

Figure 3.

MM2 energy-minimized 3D models of the aglycones of 1 (right) and 5 (left) without the C-3 sugar moiety. The chemical shifts of the protons in red are shifted upfield (shielded), while those of the protons in green are shifted downfield (deshielded) by the hydroxylation at position C-25.

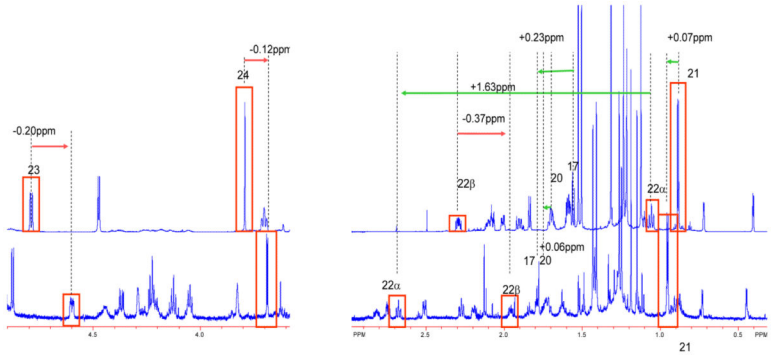

Figure 4.

^{1}H NMR spectra (900 MHz) of 5 (top) and 1 (bottom) allowed the direct comparison of (de)shielding SCS effects in the 23*R*,24*S*-and 23*R*,24*R*-type skeletons. At +1.63 ppm, H-22α exhibits the greatest overall change in chemical shift. See the main text for further discussion.

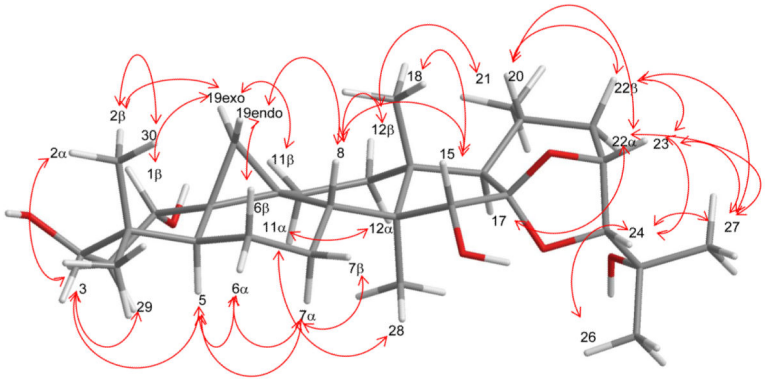

Figure 5.
Key ROESY interactions in the aglycone portion of 1.

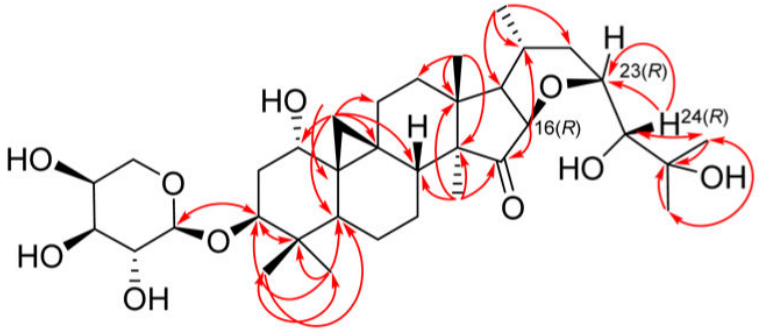

Figure 6.
Key observed HMBC correlations (H → C) for **2**.

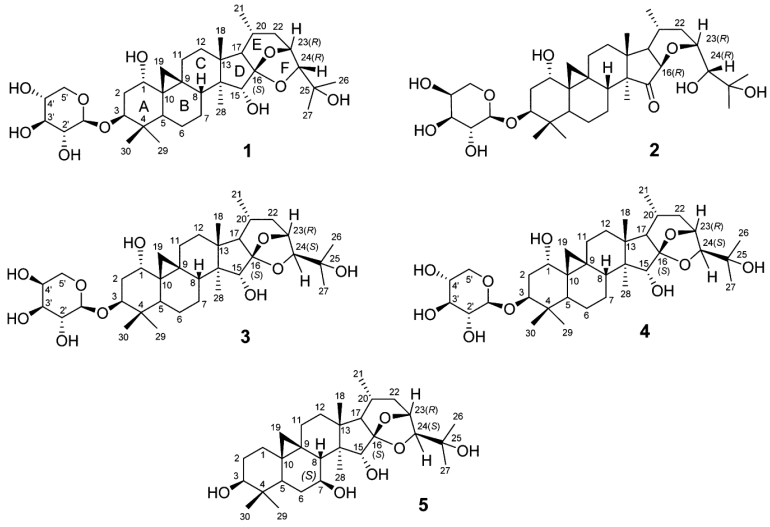

Chart 1.

Table 1

Summary of the HiFSA Iterative Analysis of the ^{1}H,^{1}H *J* Coupling Constants in the Arabinopyranose (ara*p*) and Xylopyranoside (xyl*p*) Residues in Compounds 2 and 4, Respectively

		iterated *J* coupling constants					
ara*p* (2)	multiplicity	H-1′	H-2′	H-3′	H-4′	H-5′α	H-5′β
H-1′	d		7.11	0	0	0	0
H-2′	dd	7.11		8.38	0	0	0
H-3′	dd	0	8.38		3.52	0	0
H-4′	ddd	0	0	3.52		2.91	1.61
H-5′α	dd	0	0	0	2.91		−12.40
H-5′β	dd	0	0	0	1.61	−12.40	

		iterated *J* coupling constants								
xyl*p* (4)	multiplicity	H-1′	H-2′	H-3′	H-4′	H-5′α	H-5′β	OH-2′	OH-3′	OH-4′
H-1′	d		7.55	0	0	0	0	0	0	0
H-2′	ddd	7.55		8.82	0	0	0	4.49	0	0
H-3′	ddd	0	8.82		−8.55	0	0	0	1.20	0
H-4′	dddd	0	0	−8.55		9.82	5.37	0	0	−2.74
H-5′α	dd	0	0	0	9.82		−11.38	0	0	0
H-5′β	dd	0	0	0	5.37	−11.38		0	0	0
OH-2′		0	4.49	0	0	0	0		0	0
OH-3′		0	0	1.20	0	0	0	0		0
OH-4′		0	0	0	−2.74	0	0	0	0	

J Nat Prod. Author manuscript; available in PMC 2017 March 25.

Table 2

Coupling Constants (*J*) in the Four Discrete Spin Systems of Triterpene 1 As Determined by HiFSA

	***J* [Hz]**							
spin system 1	**H-23**	**H-24**	**H-22*α***	**H-22*β***	**H-17**	**H-20**	**Me-21**	
H-23		4.16	2.26	9.80	0	0	0	
H-24	4.16		0	0	0	0	0	
H-22α	2.26	0		−13.16	0	11.44	0	
H-22*β*	9.80	0	−13.16		0	6.84	0	
H-17	0	0	0	0		10.91	0	
H-20	0	0	11.44	6.84	10.91		6.48	
Me-21	0	0	0	0	0	6.48		
spin system 2	**H-18**	**H-12*α***	**H-12*β***	**H-11*α***	**H-11*β***			
H-18		0	0.76	0	0			
H-12α	0		13.30	12.00	2.70			
H-12*β*	0.76	13.30		2.30	2.30			
H-11α	0	12.00	2.30		14.70			
H-11*β*	0	2.70	2.30	14.70				
spin system 3	**H-8**	**H-19 *endo***	**H-19 *exo***	**H-7*α***	**H-7*β***	**H-6*α***	**H-6*β***	**H-5**
H-8		0	0	12.85	3.14	0	0	0
H-19 *endo*	0		−4.31	0	0	0	0	0
H-19 *exo*	0	−4.31		0	0	0	0	0.80
H-7α	−12.85	0	0		−12.75	14.34	2.61	0
H-7*β*	3.14	0	0	−12.75		2.65	3.73	0
H-6*α*	0	0	0	14.34	2.65		−12.64	12.59
H-6*β*	0	0	0	2.61	3.73	−12.64		4.60
H-5	0	0	0.80	0	0	12.59	4.60	
spin system 4	**H-3**	**H-2*α***	**H-2*β***	**H-1**	**OH-1**			
H-3		4.45	12.00	0	0			
H-2α	4.45		−13.10	3.65	0			
H-2*β*	12.00	−13.10		2.70	0			
H-1	0	3.65	2.70		3.67			

Table 3

NMR Data (900 and 700 MHz ^{1}H) for 1

position		δ_C		δ_H, mult., *J* in Hz[b]		HMBC (H→C)	COSY	ROESY
1	*β*	72.7	3.825	brs			2*α*/*β*	2*α*,19 *exo*
2	*β*	37.8	2.272	dt	2.3, 12.7		2*α*, 1*β*, 3	19 *exo*, 30
2	*α*	37.8	2.741	dt	12.7, 3.7		2*β*, 1*β*, 3	3
3		84.6	4.366	dd	4.2, 11.7		2*α*/*β*	29, 5, 2*α*
4		41.6						
5		40.1	2.508	dd	2.5, 12.6		6*α*	6*α*, 7*β*, 3
6	*β*	20.9	0.901	overlapped			6*β*, 5,7*β*	19 *endo*
6	*α*	20.9	1.721	overlapped			7*α*, 5	5
7	*β*	26.4	1.423	overlapped			7*α*, 8	5, 7*α*
7	*α*	26.4	2.193	overlapped			6*α*, 7*β*, 8	7b, 6*α*, 8
8		49.1	1.787	dd	4.2, 12.5		7*α*	19 *endo*, 6*β*, 2*β*, 15
9		*a*						
9		*a*						
11	*β*	26.3	1.429	overlapped	6.0, 11.3		11*α*, 12*α*/*β*	19 *exo*, 11*α*
11	*α*	26.3	2.814	ddd	14.7		11*β*, 12*α*/*β*	28, 11b, 12*α*
12	*β*	34.1	1.620	overlapped			11*α*, 12*α*	21, 18
12	*α*	34.1	1.707	overlapped			11*α*, 12*β*	11*α*
13		41.8						
14		47.8						
15		81.0	4.291	d	6.8			18,8
16		112.4						
17		60.8	1.781	d	10.8			22*α*
18	Me	19.5	1.246	s		12, 13,14, 17		15
19	*exo*	30.6	0.447	d	4.2		19 *endo*	11*β*, 2*β*, 1*β*1
19	*endo*	30.6	0.729	d	4.2		19 *exo*	6*β*, 30, 8
20		23.3	1.743	m			22*α*	22*β*
21	Me	19.4	0.952	d	6.5	20, 22,17	20	12*β*, 22*α*, 22*β*
22	*β*	29.6	1.954	m			22*α*, 23	21, 17
22	*α*	29.6	2.675	dt	12.1, 1.6		22*β*, 20, 23	20, 21, 27
23		73.8	4.598	dt	12.1, 1.6	3	22*α*/*β*, 24	
24		84.1	3.685	d	6.8			
26	Me	30.7	1.406	s		27, 25, 24		24
27	Me	25.9	1.262	s		26, 25, 24		22*α*, 22*β*, 23, 24
28	Me	11.6	1.186	s		13, 8, 14, 15		11*α*
29	Me	25.7	1.430	s		30, 3, 4, 5		3
30	Me	14.7	1.147	s		29, 3, 4, 5		19 *endo*, 6*β*, 2*β*
1'		107.7	4.874	d	7.3	3	2′	
2'		75.0	4.046	dd/t	7.3, 8.7		3'	

position		δ_C	δ_H, mult., *J* in Hz[b]		HMBC (H→C)	COSY	ROESY
3'		78.7	4.123	dd/t	8.7	4'	
4'		71.4	4.206	m			
5'	*α*	67.1	3.561	dd	9.5, 11.4	*5′ β*	
5′	*β*	67.1	4.228	dd	5.3, 11.4		

[a] δ_C could not be obtained due to insufficient signal intensity.

[b] Coupling patterns given as line distances (first-order assumptions); for a detailed interpretation of the xylp ^{1}H spin system, see the data for 4 in Table 1.

Table 4

Estimated Internuclear Distances of Key Protons and Key ROE Correlations Observed for 1 (23*R*,24*R* Type) and 4 (23*R*,24*S* Type)[a]

internuclear distances in 1 [Å]		internuclear distances in 4 [Å]	
24–23	**2.1**	24–23	2.9
24–22*α*	3.9	24–22*α*	**2.2**
24–22*β*	4.3	24–22*β*	3.7
24–17	4.2	24–17[b]	**2.6**
24–20	4.9	24–20	4.4
24–26	**2.6, 3.2, 3.8**	24–26[b]	**2.4, 3.0, 3.6**
24–27	**2.8, 2.8, 3.8**	24–27[b]	**3.9, 3.1, 4.5**
24–15	4.4	24–15	5.0
22*α*–27	**2.4, 3.1, 3.8**	22*α*–27	3.5, 3.7, 4.7
22*β*–27	**3.2, 4.1, 4.9**	22*β*–27	3.9, 4.9, 5.6

[a] Calculated values for the H,H distances were obtained from a 3D model; ROE correlation cross-peaks observed in the ROESY spectra are shown in bold.

[b] Ambiguous distances due to overlapping ROE cross-peaks.

Table 5

NMR Spectroscopic Data for 2 (900 and 600 MHz ^{1}H)

position	proton	δ_C		δ_H, mult., *J* in Hz		HMBC (H→C)	COSY
1		71.9	3.777	brs		10	2*α*/*β*
2	*α*	37.3	2.738	dt	13.3, 4.1	10,4,3	2*β*, 1, 3
2	*β*		2.233	dt	2.7, 12.7		2*α*, 3
3		83.8	4.335	dd	4.5, 11.9		2*α*/*β*
4		41.1					
5		39.3	2.445	dd	12.3, 2.8	7, 10, 4,	6*α*/*β*
6	*α*	20.3	1.653	m	overlapped		6*β*,5
6	*β*		0.775	dt	12.4, 12.4		6*β*, 5,7*β*
7	*α*	25.3	2.372	m	overlapped		7*β*
7	*β*		1.352	m	overlapped		7*α*, 8
8		43.1	1.817	dd	4.3, 12.8		7*α*/*β*
9		20.8					
10		31.0					
11	*α*	25.0	2.784	m			11*β*, 12
11	*β*		1.380	m			11*α*, 12*α*/*β*
12	*α*/*β*	30.9	1.700	m			11*α*/*β*
13		39.6					
14		54.7					
15		214.5					
16		83.4	3.891	d	10.1	20, 17, 23, 15	17
17		52.6	1.574		overlapped		16
18	Me	20.1	1.252	s		12, 13, 8, 14	
19	endo	30.68	0.689	d	4.5	9, 11, 10, 8, 1	19*β*
19	exo	30.7	0.416	d	4.5	9, 11, 10, 8, 1	19*α*
20		32.5	1.860	ddt	3.9, 6.1, 10.5		21Me, 22*α*
21	Me	20.1	0.959	d	6.7	20, 22, 17	20
22	*α*	38.0	2.356	m	overlapped		22*β*, 20
22	*β*		1.551	m	overlapped		22*α*, 23
23		81.5	4.044	ddd	2.5, 6.0, 11.4		24, 22*α*/*β*
24		78.9	3.928	d	11.4	27, 22, 25, 23	23
26	Me	20.2	1.646	s		27, 25, 14	
27	Me	26.8	1.589	s		26, 25, 14	
28	Me	17.7	1.173	s		13, 8, 14, 15	
29	Me	14.6	1.070	s		30, 5, 4, 3	
30	Me	25.5	1.375	s		29, 5, 4, 3	
1′		107.0	4.813	d	7.2	5′, 3′, 3	2′
2′		72.5	4.465	t	8.0	3′, 1′	1′, 3′
3′		74.0	4.142	dd	3.6, 9.0	1	2′, 4′
4′		68.9	4.291	brs			5′*α*/*β*, 3′

position	proton	δ_C	δ_H, mult., *J* in Hz			HMBC (H→C)	COSY
5′	*α*	66.4	4.213	dd	2.9, 12.3	*4′, 3′,* 1′	5′*β*, 4′
5′	*β*		3.661		1.7, 12.3		5′*α*, 4′